

## High-pressure equation of state for solid xenon\*

K. Syassen<sup>†</sup> and W. B. Holzapfel

*Max-Planck-Institut für Festkörperforschung, 7000 Stuttgart 80, Federal Republic of Germany*

(Received 11 July 1978)

High-pressure x-ray-diffraction techniques have been used to determine the equation of state of solid xenon up to 110 kbar at 85 K. The 0-K isotherm is derived from the experimental data within the Debye approximation. The results indicate that solid Xe is much more compressible than one would expect on the basis of known pair potentials for free Xe atoms and known many-atom interactions of the Van der Waals type. The difference in compression energy between the experimental and the predicted pressure-volume relation amounts to about 30% at 100 kbar. A comparison of the experimental data with bulk properties calculated from energy-band theory by Trickey *et al.* yields good agreement. An effective pair potential for the solid state is derived from the experimental pressure-volume relation.

### I. INTRODUCTION

The cohesive energy of rare-gas solids (RGS) amounts to at most 1.5% of the atomic ionization energy. Consequently, the interaction between atoms of a RGS can be described in first approximation by pairwise additive central forces. However, a quantitative model for the cohesive properties cannot neglect many-atom interactions. Two different approaches have been used to calculate the ground-state energy of RGS and its volume dependence. In an atomic model the potential-energy function for the motion of the nuclei is determined in a semiempirical way from experimental data, quantum-mechanical calculations of the long-range Van der Waals interactions, and from assumptions on the short-range repulsive forces. This approach has led to the determination of very accurate interatomic potentials for rare-gas atoms, and successfully describes solid-state properties under near-normal conditions.<sup>1</sup> The second, more fundamental, approach is the calculation of the ground-state energy within the context of energy-band theory.<sup>2</sup>

The various models can be tested experimentally by measuring the equation of state (EOS) at high pressures. Moreover, the high-pressure EOS is a bulk property which yields direct information on overlap-dependent many-atom interactions. Since many-body interactions increase from neon to xenon, we have chosen Xe to study its EOS.

Furthermore, among the RGS Xe is of particular interest, because it is expected to transform to the metallic state at the lowest pressure, discarding Rn for obvious reasons. Estimates for the transition pressure vary between 700 kbar (Ref. 3) and several Mbar.<sup>4</sup> The situation here is somewhat similar to the expected insulator-metal transition of solid hydrogen under pressure<sup>5</sup>: The knowledge of the EOS of the molecular state is an

essential information for the calculation of the transition pressure.

Another aspect of the EOS of solid Xe is its relation to the Thomas-Fermi-Dirac (TFD) theory. Xe is the heaviest stable atom with a closed electron configuration and low binding energy. Therefore, solid Xe should be the best candidate to be described by the statistical theory of atoms.

Experimentally, the high-pressure EOS of Xe has been studied by two different methods: by direct volume measurements up to 20 kbar,<sup>6,7</sup> and by shock compression up to about 500 kbar.<sup>8</sup> Piston-displacement techniques are presently limited in pressure to some 10 kbar. The problems involved in the shock-wave experiment, e.g., limited accuracy and high temperature, make it difficult to obtain information on the low-temperature isothermal pressure-volume ( $P$ - $V$ ) relation. The present work is a first step to extend the EOS measurements on RGS to higher static pressures using x-ray diffraction techniques.

The experimental technique for x-ray diffraction studies at high pressures and low temperatures is described briefly in Sec. II. The present experimental results for the 85-K isotherm of Xe up to 108 kbar are presented in Sec. III. In Sec. IV we derive the pressure dependence of the ground-state energy ( $T=0$  K), discuss the importance of many-atom interactions, present an "effective" pair-potential for Xe in the solid state, and, finally, compare the experimental data with the TFD theory.

### II. EXPERIMENT

The high-pressure x-ray diffraction technique used in this study has been described in detail elsewhere.<sup>9</sup> Here, we only recall the basic features of the high-pressure cell as shown in Fig. 1. The cell consists of one tungsten-carbide anvil and one boron-carbide anvil. Both anvils are pre-

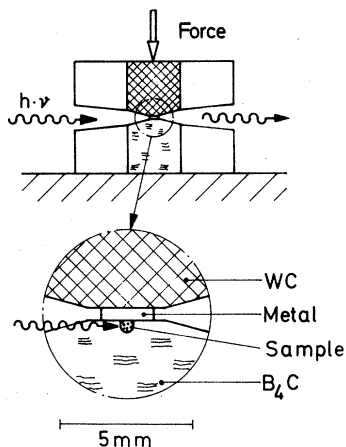


FIG. 1. Schematic drawing of the high-pressure cell.

stressed by supporting rings. The inset in Fig. 1 elucidates the details of the pressure cell. The sample is filled into a small hole (0.4-mm diam and 0.5-mm depth) within the tip of the boron-carbide anvil. By squeezing the two anvils together, the metal disk starts to deform and a pressure gradient develops across the metal disk with maximum pressure in the center just above the sample. The metal then flows into the sample hole and pressurizes the sample. X rays pass through the boron-carbide anvil just below the metal disk. The scattered radiation is recorded in the plane perpendicular to the anvil axis.

The temperature is measured by a Pt resistor which is directly attached to the tungsten-carbide anvil. The pressure measurement is based on the use of a marker substance, in this case either NaCl or Al. The EOS for both substances is known at room temperature.<sup>10,11</sup> Low-temperature  $P$ - $V$  relations are derived from known thermodynamic properties and an assumption about the volume dependence of the Grüneisen parameter. The  $P$ - $V$  relations are calculated in the Appendix.

The procedure for sample preparation is as follows. First, the sample volume in the boron-carbide anvil is completely filled with the marker substance. Then a cylindrical hole of 0.1-mm diam is drilled into the center of the marker substance. Xenon of 99.99% purity is directly condensed into this little hole at about 150 K without being in contact with other gases. Finally, the precooled high-pressure unit is assembled at 77 K and transferred into the cryostat. A more detailed account of the sample preparation procedure is given elsewhere.<sup>12</sup>

The x-ray diffraction patterns of fcc xenon were measured at 85 K under pressures between 1 bar

and 108 kbar. Altogether, seven samples were prepared, two with NaCl and five with Al as marker substance. On an average, five different reflections have been obtained per substance. However, the number of evaluated lines was sometimes smaller due to overlap of reflections or interference with the diffraction pattern of the boron-carbide anvil.

Experimental lattice parameters for Al and Xe measured in the high-pressure cell at 1 bar and 85 K agree with values derived from known densities and thermal-expansion coefficients to within a relative deviation of  $2 \times 10^{-4}$  (for Al: experimental,  $4.0328 \pm 0.0015$  Å; calculated,  $4.0335$  Å,<sup>13</sup> and for Xe: experimental,  $6.2166 \pm 0.002$  Å; calculated  $6.2164$  Å.<sup>14-16</sup>

### III. RESULTS

The experimental  $P$ - $V$  data for solid Xe at 85 K are shown in Fig. 2. The solid dots refer to measurements with Al as internal-pressure marker and the solid triangles to data with NaCl as marker. The solid line corresponds to a least-squares fit of a Keane equation<sup>17,18</sup> to the data points:

$$P(V) = (B_0 B'_0 / B_\infty'^2) [(V_0/V)^{B_\infty} - 1] - [B_0(B'_0 - B_\infty') / B_\infty'] \ln(V_0/V). \quad (1)$$

Here,  $B_0$  and  $B'_0$  are the isothermal bulk modulus and its pressure derivative at normal pressure.  $B_\infty'$  is the pressure derivative of the bulk modulus

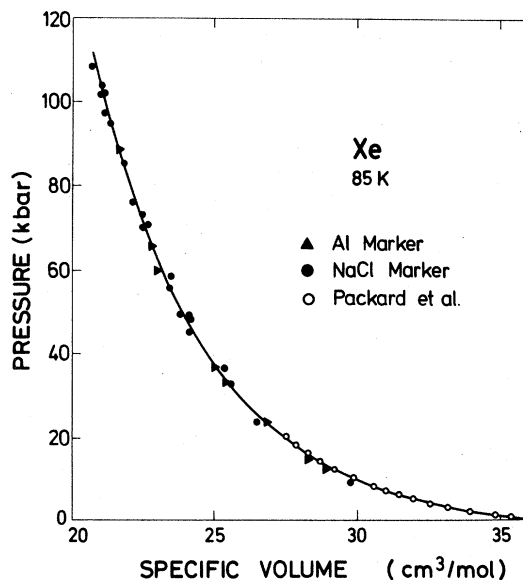


FIG. 2. Experimental  $P$ - $V$  relation for solid Xe at 85 K. For comparison, the data of Packard and Swenson (see Ref. 6) are included.

TABLE I. Parameters for the Keane equation [Eq. (1)] representing the  $P$ - $V$  relations of solid Xe at 85 K, 0 K, and in the static-lattice limit.

$T$	$V_0$ (cm <sup>3</sup> /mol)	$B_0$ (kbar)	$B'_0$	$B'_\infty$
85 K	36.17 <sup>a</sup>	26.5 <sup>d</sup>	7.69	4.80
0 K	34.72 <sup>b</sup>	36.48	6.83	4.80
Static lattice	34.33 <sup>c</sup>	38.14	6.88	4.81

<sup>a</sup> Extrapolated using lattice parameters and thermal-expansion coefficients given in Refs. 14–16.

<sup>b</sup> From Ref. 14.

<sup>c</sup> Calculated from the 0-K isotherm and  $P_{ZP}(V)$ .

<sup>d</sup> From Refs. 7 and 19. See text.

at high pressure, and  $V_0$  is the volume at normal pressure. The value of  $B_0$  depends strongly on low-pressure data. The piston-displacement data of Anderson and Swenson<sup>7</sup> and the ultrasonic results by Bezuglyi *et al.*<sup>19</sup> give the same value of  $B_0 = 26.5$  kbar at 85 K. Since there are no x-ray data in the low-pressure region, we adopted this number as a constant parameter for the least-squares fit. Results for  $B_0$ ,  $B'_0$ , and  $B'_\infty$  are listed in Table I. For comparison, the smoothed  $P$ - $V$  relation from piston cylinder studies by Packard and Swenson<sup>6</sup> is included in Fig. 2. Their data show a better agreement with the present x-ray data than the more recent piston-cylinder results by Anderson and Swenson.<sup>7</sup> The reason for the difference between the two direct volume measurements is not clear.<sup>7</sup>

The scatter of the individual data points with respect to the average  $P$ - $V$  curve in Fig. 2 is definitely larger than the systematic error of the x-ray-diffraction technique. This can be explained by the nonisostatic pressure conditions in the present pressure cell. Lattice-parameter measurements with the incident and diffracted x-ray beam normal to the direction of the piston motion underestimate the relative volume change.<sup>20,21</sup> The deviation from the volume change corresponding to a truly isostatic compression depends on the size of the uniaxial stress component, on the elastic properties of the material under pressure, on the  $(hkl)$  value of the reflection used to evaluate lattice parameters, and on the geometry of the pressure cell.<sup>20</sup> The uniaxial stress component varies from run to run depending on the sample composition. Also, it is not possible to always use the same set of reflections for calculating lattice parameters. Therefore, we find a relatively large scatter of the data points.

From the above explanation, it also follows that an average  $P$ - $V$  relation measured by the present

technique always shows a systematic error, because, in general, the structural and elastic properties of marker and sample are different. The width of the scatter of the data points around the average  $P$ - $V$  relation gives an estimate of the maximum systematic error. This statement can be supported as follows: (i) Test runs in the present high-pressure cell with NaCl as “sample” and Al as “marker” and vice versa yield agreement of both  $P$ - $V$  relations to within less than  $\pm 1.5$  kbar. Therefore, both substances “feel” almost the same pressure, independent of the geometrical arrangement within the pressure cell. (ii) For the Xe experiment there is no systematic deviation using NaCl or Al as a pressure marker, though the elastic properties of both substances are quite different.

Taking into account the uncertainty of the EOS of Al (which is based on the EOS of NaCl), we estimate that the average  $P$ - $V$  curve through the data points in Fig. 2 has a maximum systematic error of  $\pm 4$  kbar at 100 kbar with respect to the NaCl pressure scale.

#### IV. DISCUSSION

Starting from the experimental  $P$ - $V$  relation, we will first determine the EOS for the ground state at 0 K and in the static-lattice limit. Comparison with known free-atom Xe-Xe interactions gives us information on short-range many-atom effects. We will also compare the experimental results with energy-band calculations of the  $P$ - $V$  relation. From the volume dependence of the ground-state energy, we will then derive an “effective” interatomic pair potential for the solid state. Finally, we add some remarks on the TFD theory and on the insulator-metal transition of solid xenon.

##### A. Ground-state $P$ - $V$ relation

For the derivation of the ground-state  $P$ - $V$  relation we will use some thermodynamic relations, which are summarized here briefly.

In the Mie-Grüneisen approximation the EOS can be written<sup>22,23</sup>

$$\begin{aligned}
 P(V, T) &= -[\partial F(V, T)/\partial V]_T \\
 &= P_{SL}(V) + \gamma'(V)E_{\text{vib}}(V, T)/V \\
 &= P_{SL}(V) + P_{ZP}(V) + P_{TH}(V, T). \quad (2)
 \end{aligned}$$

$F$  is the Helmholtz free energy,  $E_{\text{vib}}(V, T)$  is the total vibrational energy,  $\gamma'$  is a Grüneisen parameter, and  $P_{SL}$ ,  $P_{ZP}$ , and  $P_{TH}$  are potential pressure in the static-lattice limit, zero-point pressure and thermal pressure, respectively.

We assume that  $\gamma'$  does not depend on temperature. In the vibrational formulation of the Mie-Grüneisen approximation<sup>22</sup> one identifies  $\gamma'$  with the parameter  $\gamma$  defined by the Grüneisen relation

$$\gamma = \beta VB/c_V, \quad (3)$$

where  $\beta$ ,  $B$ , and  $c_V$  are the coefficient of volume thermal expansion, isothermal bulk modulus, and heat capacity at constant volume, respectively.

In the Debye approximation we find for the zero-point pressure  $P_{ZP}(V)$  and the thermal pressure<sup>23</sup>  $P_{TH}(V, T)$

$$P_{ZP}(V) = \gamma 9Nk\Theta/8V, \quad (4)$$

$$P_{TH}(V, T) = \gamma(3NkT/V)D(\Theta/T), \quad (5)$$

where  $N/V$  is the number of atoms per unit volume and  $D(\Theta/T)$  is the Debye function.<sup>13</sup> The Debye temperature  $\Theta$  is related to  $\gamma$  by

$$\gamma(V) = -d \ln \Theta(V)/d \ln V, \quad (6a)$$

or

$$\Theta(V) = \Theta(V_0) \exp \int_{V_0}^V \frac{\gamma}{V} dV. \quad (6b)$$

The actual form of the volume dependence of  $\gamma$  is not known.

Holt and Ross<sup>24</sup> suggest, on the basis of several model calculations, that a linear relationship

$$\gamma(V) = \gamma_1(V/V_0) + \gamma_\infty \quad (7)$$

should be an appropriate approximation for closed-shell systems.  $\gamma_\infty$  is the limiting value of  $\gamma$  at  $V \rightarrow 0$ . We follow Kopyshv<sup>25</sup> and Holt and Ross,<sup>24</sup> and assume  $\gamma_\infty = \frac{1}{2}$ . The constant  $\gamma_1$  can be determined from the known  $\gamma$  at  $V = V_0$ .

For Xe the specific volume  $V_0(85 \text{ K})$  at 1 bar and 85 K is  $36.17 \text{ cm}^3/\text{mol}$ .<sup>14-16</sup>  $\gamma(V_0(85 \text{ K}))$  derived from thermal-expansion measurements using Eq. (3) is 2.86.<sup>15</sup> From specific-heat measurements<sup>26</sup> we find  $\Theta(V_0(85 \text{ K})) = 57 \text{ K}$ . Figure 3 shows the volume dependence of the thermal pressure  $P_{TH}(V, 85 \text{ K})$  calculated according to Eqs. (5)–(7) using the above values for  $V_0(85 \text{ K})$ ,  $\gamma(V_0(85 \text{ K}))$ , and  $\Theta(V_0(85 \text{ K}))$ . The thermal pressure at  $V_0^0 = V(1 \text{ bar}, 0 \text{ K}) = 34.72 \text{ cm}^3/\text{mol}$  amounts to 1.26 kbar and is in excellent agreement with the pressure calculated from the Keane equation with parameters for 85 K given in Table I. This adds some confidence to the choice of the values for  $\gamma(V_0(85 \text{ K}))$  and  $\Theta(V_0(85 \text{ K}))$ . In the calculation of  $P_{ZP}(V)$ —also shown in Fig. 3—we used the same relations for  $\gamma(V)$  and  $\Theta(V)$  in order to keep our model consistent. We have to bear in mind, however, that in reality  $\gamma$  and  $\Theta$  also depend on temperature. This may cause an estimated error of about 10% for the calculated  $P_{ZP}(V_0^0)$ . The value of  $\Theta(V_0^0) = 64$

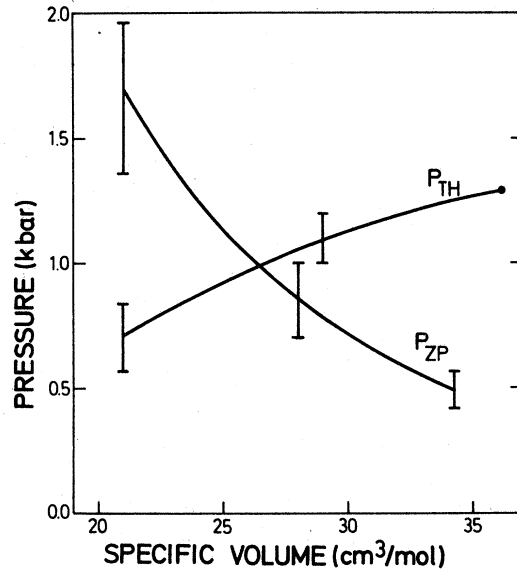


FIG. 3. Thermal-pressure  $P_{TH}$  (at 85 K) and zero-point pressure  $P_{ZP}$  for solid Xe. Error bars are estimated.

K determined from specific-heat measurements<sup>27</sup> coincides with the calculated  $\Theta(V)$  relation.

Errors in  $P_{TH}$  and  $P_{ZP}$  are mainly caused by the uncertainty in the volume dependence of  $\gamma$ . We estimate these errors to be  $\pm 0.1$  kbar for  $P_{TH}$  and  $\pm 0.3$  kbar for  $P_{ZP}$  at 120 kbar. In view of the accuracy of the experimental data, the use of a rather simple model for the volume dependence of  $P_{TH}$  and  $P_{ZP}$  is justified.

We can now construct the 0-K isotherm and the  $P$ - $V$  relation in the static-lattice limit from the average  $P$ - $V$  relation at 85 K according to Eq. (2). The corresponding parameters for the Keane equation are also given in Table I.  $B_0(0 \text{ K}) = 36.5$  kbar compares quite well with the extrapolated bulk moduli 36.1, 36.5, and 36.7 kbar from, respectively, ultrasonic,<sup>19</sup> piston displacement,<sup>7</sup> and inelastic neutron scattering<sup>28</sup> experiments. The agreement is less favorable for the value 37.9 kbar given by Korpium *et al.*<sup>29</sup>  $B_0$  increases slightly in going from 0 K to the static-lattice limit.  $B_\infty$  essentially stays the same for all three  $P$ - $V$  relations. For the remainder of the discussion we will concentrate on the 0-K isotherm.

### B. Many-body interactions

Interatomic potentials for the ground state of two rare-gas atoms have been determined quite accurately in a semiempirical way.<sup>1</sup> The potentials are based on known long-range interactions of the

Van der Waals type and on a wide range of experimental data like gas transport properties, second virial coefficients, spectroscopic information on dimers, and differential scattering cross sections. In order to determine the depth and the position of the potential minima, solid-state data, such as cohesive energy and lattice spacing at normal pressure, have been used after taking into account contributions from many-atom Van der Waals interactions. Potentials of this type agree essentially with all strictly two-body experimental information and also with condensed-phase data. However, it was already pointed out<sup>30</sup> that there exists a small discrepancy for the cohesive energy of solid Xe. Nevertheless, the assumption was made that *overlap dependent many-atom interactions can be neglected for all RGS at normal pressure*,<sup>30</sup> and that the Barker potential<sup>30</sup> for Xe should be reasonable to an energy of  $3 \times 10^{-20}$  J.<sup>31</sup> The equivalent interatomic spacing in the solid would correspond to pressures of several hundred kilobars.

If the assumption concerning overlap-dependent many-body interactions is valid, it seems appropriate to determine the EOS of Xe from the interatomic potential by including higher-order Van der Waals terms. The  $P$ - $V$  relation for Xe at 0 K calculated by Barker<sup>31</sup> using potential X3,<sup>30</sup> with third-order  $DDD$ ,  $DDQ$ ,  $DQQ$ ,  $QQQ$ , and fourth-order  $DDD$  interactions ( $D$ : dipole;  $Q$ : quadrupole), is shown in Fig. 4 together with the "experimental" 0-K isotherm. A comparison between the two  $P$ - $V$  relations reveals that Xe is much more compressible than expected on the basis of the free-atom

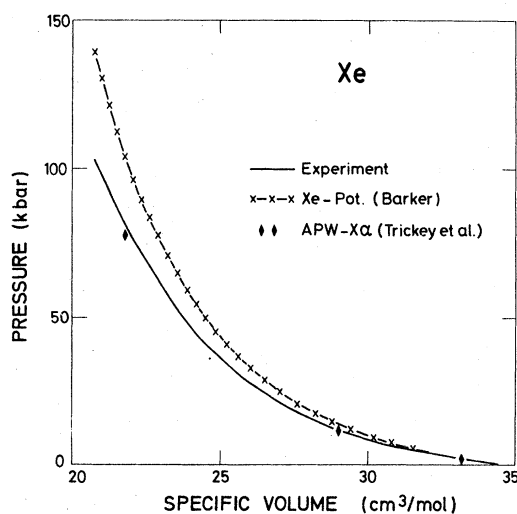


FIG. 4. Comparison of experimental and theoretical  $P$ - $V$  relations of solid Xe at 0 K. (Barker, Ref. 31; Trickey *et al.*, Ref. 2.)

Xe-Xe potential. The difference in the energy of compression amounts to about 30% at  $21 \text{ cm}^3/\text{mol}$  (100 kbar) relative to the experimental EOS. The absolute numbers are 0.37 and 0.48 eV/atom, respectively. For comparison, the cohesive energy at 1 bar is 0.164 eV/atom.<sup>32</sup> This means that the total lattice energy at  $21 \text{ cm}^3/\text{mol}$  is lower by about 17% relative to the Barker EOS. We can conclude that *overlap-dependent many-atom interactions contribute a considerable amount to the total lattice energy of Xe in the 100-kbar region*. In view of this result, it seems obvious that the small discrepancy between the cohesive energy at 1 bar and the corresponding value derived from the Barker potential may also result from short-range many-atom interactions.<sup>33</sup>

An interpretation of the overlap-dependent interactions can be given either in atomic terms or in the energy-band picture. An appropriate atomic model has been discussed by Niebel and Venables<sup>34</sup> in their attempt to explain the crystal structure of RGS. One can adopt their arguments to explain the additional attractive interaction in compressed Xe. Briefly, the excited-state wave functions of an atom in the crystal overlap considerably with the neighboring atoms. In a first approximation this effect can be described by a crystal-field perturbation.

In fcc Xe the main effect of the crystal field is to split the degenerate energy levels of the  $5d$  orbitals. This is obvious, because the  $5d-t_{2g}$  orbitals point towards nearest neighbors, whereas the  $5d-e_g$  orbitals point into the space between the neighbors. This perturbation leads to a decrease of the energy difference between the first excited state and the highest valence state. As a consequence, the leading dipole-dipole term of the attractive Van der Waals interaction is expected to increase in the solid with respect to the free atom interaction in the gas phase. By applying pressure to the crystal, this effect is enhanced, thereby adding attractive interaction to the total lattice energy and increasing the compressibility. A quantitative calculation of the Van der Waals energy and its dependence on interatomic spacing within this localized atomic model of the solid is expected to account for most of the difference between the Barker EOS and the present experimental data.

The localized model will become less valid with increasing overlap of the excited-state wave functions.<sup>35</sup> A calculation of the Van der Waals interaction based on electron-band states and energies will become more appropriate with increasing pressure. Within such a band picture the additional attractive interaction is explained qualitatively in a similar way. The width of the bands increases

with decreasing interatomic separation, thereby lowering the energy gap between the  $5p$  valence and the  $5d$  excited states. Again one anticipates an increase of the attractive Van der Waals interaction.

The starting point in the above discussion was the semiempirical Xe-Xe potential for free atoms. So far, we considered only the *difference* between the Barker EOS and the experimental 0-K isotherm. Therefore, our interpretation of the experimental data is still based on atomic terms and has a semiempirical character. A more fundamental approach is the calculation of the total ground-state energy of Xe from energy-band theory. An attempt of this type has been reported by Trickey *et al.*<sup>2</sup> Using the APW- $X\alpha$  method, they calculated the volume dependence of the ground-state energy (0 K). The corresponding  $P$ - $V$  data are included in Fig. 4. We find a very good agreement between these theoretical and the present experimental data. This result supports the conclusion given by Trickey *et al.* that the APW- $X\alpha$  model may be a successful approach for first-principle calculations of the bulk properties also in the case of RGS. It leads beyond the scope of the present work to discuss this point any further. However, we would like to point out that calculations of this type may be very appropriate for an extrapolation of the EOS to smaller volumes and higher pressures.

### C. Effective pair potential

Lattice dynamics and thermodynamic properties of solid Xe depend in various ways on details of the

interatomic potential. From the experimental  $P$ - $V$  relation we can determine an "effective" pairwise additive potential which includes many atom interactions. We start from an analytical form similar to the Barker pair potential<sup>30</sup>:

$$U(r) = \epsilon \left( [A_0 + A_1(r-1)] e^{\alpha(1-r)} - \sum_i \frac{C_i}{r^i} + \frac{C_9}{r^9} \right) \quad (8)$$

with

$$r = R/\sigma, \quad i = 6, 8, 10$$

$R$ ,  $\epsilon$ , and  $\sigma$  are interatomic separation, depth of the potential, and position of the potential minimum, respectively. The first term describes the repulsive part of the potential. The second summation corresponds to the long-range Van der Waals terms ( $DD$ ,  $DQ$ , and  $QQ$ ). For the coefficients  $C_i$  we have adopted the recent values given by Doran.<sup>35</sup> The third ( $r^{-9}$ ) term stands for the  $DDD$  interaction. The constant  $C_9$  is calculated from the third-order  $DDD$  interaction constant and the corresponding geometric factor for the fcc lattice given in Refs. 35 and 36. The constants  $A_0$  and  $A_1$  are determined through the choice of the constants  $C_i$  via the relations  $U(r=1) = -\epsilon$  and  $U'(r=1) = 0$ . The only adjustable parameters left are  $\epsilon$ ,  $\sigma$ , and  $\alpha$ .

The total cohesive energy is calculated by summation over the fcc lattice. By fitting the lattice sum to the experimental ground-state energy at 0 K [ $E(V) = -\int_{V_0}^V P dV + E(V_0)$ , with  $E(V_0)$  for the cohesive energy at normal pressure], we find the values of  $\epsilon$ ,  $\sigma$ , and  $\alpha$  as summarized in Table II. The differences in  $\epsilon$ ,  $\sigma$ , and  $\alpha$  between the Barker potential and the present potential reflect the con-

TABLE II. Comparison of parameters for the pairwise additive interatomic potential of Xe in the solid state and in the gas phase. Not listed are some additional parameters of the free-atom Xe-Xe potential (see Ref. 30).

	Solid, 0 K	Static lattice	Free atom <sup>a</sup>
$E(V_0)$ ( $10^{-23}$ J/atom)	2632 <sup>b</sup>	2733 <sup>c</sup>	2663
$\epsilon$ ( $10^{-23}$ J)	346.22	360.18	389.96
$\sigma$ (Å)	4.4287	4.4091	4.3623
$\alpha$	10.2	10.2	12.5
$C_6$	1.0298 <sup>d</sup>	1.0298 <sup>d</sup>	1.0544
$C_8$	0.3679 <sup>d</sup>	0.3679 <sup>d</sup>	0.1660
$C_{10}$	0.0621 <sup>d</sup>	0.0621 <sup>d</sup>	0.0323
$C_9$	-0.1042 <sup>e</sup>	-0.1042 <sup>e</sup>	...
$A_0$	0.3553	0.3553	0.2402
$A_1$	-5.1811	-5.1811	-4.8169

<sup>a</sup> Reference 30, potential X2.

<sup>b</sup> Reference 32.

<sup>c</sup> Calculated from  $P_{ZP}(V)$  and  $E(V_0, 0 \text{ K}) = 2632 \times 10^{-23}$  J/atom.

<sup>d</sup> Reference 35.

<sup>e</sup> References 35 and 36; see text.

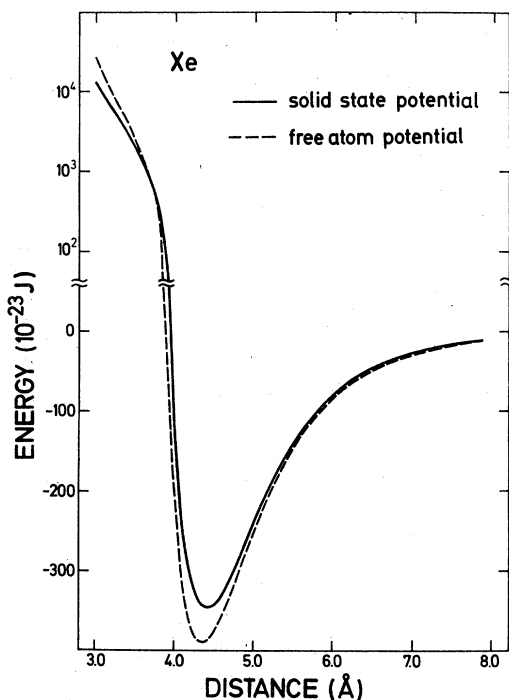


FIG. 5. Comparison of the free-atom Xe-Xe potential and the effective pair potential for the solid state.

tributions of many-atom interactions which decrease the depth of the solid-state potential, and shift the position of the potential minimum to a larger interatomic distance. The strength of the repulsive interaction given by the value of  $\alpha$  is lower in the solid state, because the overall effect of the *short-range* many-atom interactions is attractive. In order to visualize these differences, the 0-K potential and the Barker potential are shown in Fig. 5. For completeness we also list in Table II the potential parameters corresponding to the static-lattice limit. In going from 0 K to the static lattice, the depth of the potential increases by 3.5%. This agrees with the contribution of the zero-point energy to the total lattice energy calculated by Chell and Zucker.<sup>37</sup>

#### D. Comparison with Thomas-Fermi-Dirac theory

The statistical theory of atoms has been used widely to derive EOS for solids under very high pressure.<sup>38-41</sup> The TFD theory yields best agreement with experimental  $P$ - $V$  relations for the heavy atoms with closed-shell electronic configuration and low binding energy. For Xe the TFD theory predicts a pressure of 2 kbar at the experimental volume under normal conditions (1 bar, 0 K).<sup>42</sup> In general, one expects that the rela-

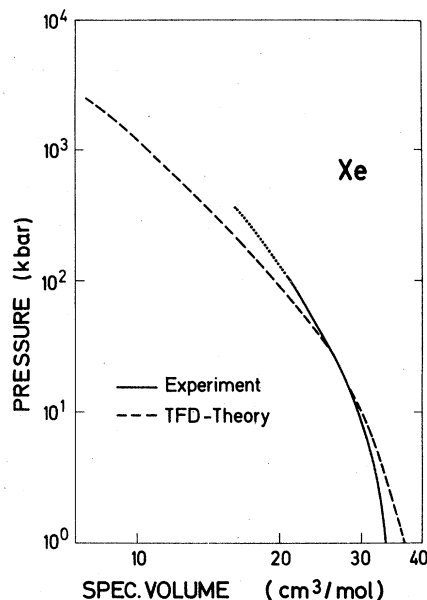


FIG. 6. Comparison of the experimental  $P$ - $V$  relation of Xe at 0 K with TFD theory.

tive accuracy of the TFD EOS improves at higher pressures. The comparison of the TFD EOS<sup>42</sup> with the present experimental data for Xe in Fig. 6 shows, however, an *increase* in the discrepancies between the TFD and experimental data under pressures in excess of 20 kbar.

Obviously, this discrepancy has a real physical significance in the case of Xe, where the closed electronic shells and the large band gap provide an extra stiffness to the electronic charge distribution of the atoms compared to a TFD model, which neglects quantum effects completely and, consequently, imposes weaker restrictions on the rearrangement of the electronic charge in the solid under pressure. Therefore, one can expect that the TFD EOS represents more accurately the behavior of metallic Xe at very high pressures. The smaller volume of Xe in this case may be considered as one of the factors which favor a first-order phase transition to the metallic state.

#### V. CONCLUSION

The results of the present experiment can be summarized as follows: (i) The  $P$ - $V$  relation for solid Xe is represented by a Keane equation with parameters given in Table I. (ii) Under pressure many-atom interactions contribute a considerable amount to the *total* lattice energy (~17% at 100 kbar). The additional attractive interaction can be explained by a variation of the long-range Van der Waals forces due to short-range overlap-de-

pendent effects. (iii) The agreement between a  $P$ - $V$  relation based on energy-band calculations of the ground-state energy by Trickey *et al.*<sup>2</sup> and the experimental 0-K isotherm is remarkably good. (iv) An "effective" interatomic pairwise additional potential for the solid state is derived which may prove useful in calculations of lattice dynamics and thermodynamic properties. (v) Due to the closed-shell structure of Xe, the TFD EOS is too soft for Xe in the insulating phase, and may represent more closely the EOS of metallic Xe under higher pressures.

It is obvious that further high-pressure studies on solid Xe in a diamond anvil device are extremely interesting. At a pressure of around 200–500 kbar, the band gap of Xe is expected to decrease below 5 eV, which is the optical absorption edge of diamond. At this point, optical studies of the pressure dependence of the excited electronic states become possible in addition to x-ray measurements. Even if the pressure corresponding to the insulator metal transition of Xe is outside the capability of the diamond anvil technique, optical studies will enable one to estimate the transition pressure more reliably.

#### ACKNOWLEDGMENTS

We are grateful to Dr. J. A. Barker for helpful correspondence and discussions. We would like to thank W. Dieterich and W. Böhringer for very skillful technical assistance. Part of the work was supported by the Deutsche Forschungsgemeinschaft.

#### APPENDIX: LOW-TEMPERATURE EOS OF NaCl and Al

The room-temperature  $P$ - $V$  relation of NaCl reported by Decker<sup>10</sup> is used as a pressure standard. From the isotherm at 298 K we obtain the  $P$ - $V$  relation at low temperature by calculating the difference in thermal pressure. We assume a linear relationship for the volume dependence of the thermal-pressure  $P_{TH}(V, T)$ :

$$P_{TH}(V, T) = P_{TH}(V_0, T) - DP_{TH}(V_0, T)(1 - V/V_0).$$

$DP_{TH}(V_0, T)$  is the quantity  $(1/V)[dP_{TH}(V, T)/dV]_T$  at normal pressure. Values for  $DP_{TH}$  have been calculated from known thermodynamic properties of the NaCl crystal by Masse.<sup>43</sup>  $P_{TH}(V_0, T)$  is taken from the isotherm at 298 K. The difference in  $P_{TH}$  between 298 K and 85 K is then given by

$$\Delta P_{TH}(V) = 5.60 - 6.80[1 - V/V_0(298 \text{ K})] \text{ kbar}.$$

TABLE III. Isothermal-compression data for NaCl and Al at 298 and 85 K. The low-temperature isotherms are used as pressure standards in the present study.

$V/V_0$	NaCl, 298 K	NaCl, 85 K	Al, 298 K	Al, 85 K
1.00	0.00	0.00	0.00	0.00
0.99	2.44	2.77	7.47	8.06
0.98	5.02	5.70	15.34	16.54
0.97	7.76	8.80	23.64	25.46
0.96	10.67	12.09	32.41	34.86
0.95	13.76	15.56	41.65	44.77
0.94	17.03	19.25	51.40	55.20
0.93	20.50	23.15	61.69	66.19
0.92	24.19	27.28	72.56	77.79
0.91	28.11	31.64	84.02	90.02
0.90	32.26	35.29	96.14	102.91
0.89	36.66	41.21	108.94	116.51
0.88	41.35	45.42	122.45	130.87
0.87	46.33	51.93	136.75	146.03
0.86	51.61	57.79	151.85	162.04
0.85	57.23	64.02	167.82	178.96
0.84	63.19	70.62		
0.83	69.54	77.63		
0.82	76.28	85.07		
0.81	83.47	92.97		
0.80	91.11	101.38		
0.79	99.25	110.31		
0.78	107.92	119.81		
0.77	117.15	129.93		
0.76	126.99	140.71		
0.75	137.48	151.39		

The room-temperature  $P$ - $V$  relation of Al, based on the EOS of NaCl, is described by a Birch equation with parameters  $B_0 = 727$  kbar and  $B'_0 = 4.3$ .<sup>11</sup> The difference in thermal pressure between 298 and 85 K is calculated within the Debye model [Eq. (5)]. We assume a linear volume dependence of  $\gamma$  which is determined by two values<sup>44,45</sup>:

$$\gamma(V_0(298 \text{ K})) = 2.15 \text{ and } \gamma(0.9V_0(298 \text{ K})) = 1.70.$$

The Debye temperature is taken as an adjustable parameter so that  $\Delta P_{TH}$  at  $V_0(85 \text{ K})$  and 85 K coincides with the value taken from the 298-K isotherm. Within the 120-kbar range, the result can be approximated by a linear relationship:

$$\Delta P_{TH}(V) = 9.15 - 20[1 - V/V_0(298 \text{ K})] \text{ kbar}$$

The isotherms of NaCl and Al for the two temperatures 298 and 85 K are tabulated in Table III. The uncertainty of the low-temperature  $P$ - $V$  relations is estimated to be  $\pm 0.5$  kbar for NaCl and  $\pm 2.0$  kbar for Al at 100 kbar relative to Decker's<sup>10</sup> room-temperature isotherm of NaCl.



- \*A preliminary report has been given in Europhys. Conf. Abstr. A 1, 87 (1975).
- †Present address: Universität Düsseldorf, Experimentalphysik III, 4000 Düsseldorf 1, Federal Republic of Germany.
- <sup>1</sup>J. A. Barker, in *Rare Gas Solids*, edited by M. L. Klein and T. R. Koehler (Academic, New York, 1975), Vol. 1, Chap. 4.
  - <sup>2</sup>S. B. Trickey, F. R. Green, Jr., and F. W. Averill, *Phys. Rev. B* 8, 4822 (1973).
  - <sup>3</sup>M. Ross, *Phys. Rev.* 171, 777 (1968).
  - <sup>4</sup>D. Brust, *Phys. Lett. A* 38, 157 (1972).
  - <sup>5</sup>R. S. Hawke, in *Festkörperprobleme XIV*, edited by H. J. Queisser (Vieweg-Verlag, Braunschweig, 1974), p. 111.
  - <sup>6</sup>J. R. Packard and C. A. Swenson, *J. Phys. Chem. Solids* 24, 1405 (1963).
  - <sup>7</sup>M. S. Anderson and C. A. Swenson, *J. Phys. Chem. Solids* 36, 145 (1975).
  - <sup>8</sup>R. N. Keeler, M. van Thiel, and B. J. Alder, *Physica (Utr.)* 31, 1437 (1965).
  - <sup>9</sup>K. Syassen and W. B. Holzapfel, *Rev. Sci. Instrum.* 49, 1107 (1978).
  - <sup>10</sup>D. L. Decker, *J. Appl. Phys.* 42, 3239 (1971).
  - <sup>11</sup>K. Syassen and W. B. Holzapfel, *J. Appl. Phys.* 49, 4427 (1978).
  - <sup>12</sup>K. Syassen, thesis (Universität Stuttgart, 1974) (unpublished).
  - <sup>13</sup>*AIP Handbook*, edited by D. E. Gray (McGraw Hill, New York, 1972).
  - <sup>14</sup>D. E. Sears and H. P. Klug, *J. Chem. Phys.* 37, 3002 (1962).
  - <sup>15</sup>C. R. Tilford and C. A. Swenson, *Phys. Rev. B* 5, 719 (1972).
  - <sup>16</sup>V. G. Manzhelii, V. G. Gavrilko, and V. I. Kuchnev, *Phys. Status Solidi* 34, K55 (1969).
  - <sup>17</sup>A. Keane, *Austr. J. Phys.* 7, 323 (1954).
  - <sup>18</sup>O. L. Anderson, *Phys. Earth Planet. Inter.* 1, 169 (1968).
  - <sup>19</sup>P. A. Bezuglyi, L. M. Tarasenko, and O. J. Baryshevskii, *Sov. Phys. Solid State* 13, 2003 (1972).
  - <sup>20</sup>A. K. Singh and G. C. Kennedy, *J. Appl. Phys.* 45, 4686 (1974).
  - <sup>21</sup>A. L. Ruoff, *J. Appl. Phys.* 46, 1389 (1975).
  - <sup>22</sup>F. G. Fumi and M. P. Tosi, *J. Chem. Phys. Solids* 23, 395 (1962).
  - <sup>23</sup>V. N. Zharkov and V. A. Kalinin, *Equations of State for Solids* (Consultants Bureau, New York, 1971), Chap. 2.5.
  - <sup>24</sup>A. C. Holt and M. Ross, *Phys. Rev. B* 1, 2700 (1970).
  - <sup>25</sup>V. P. Kopyshchev, *Sov. Phys. Dokl.* 10, 338 (1965).
  - <sup>26</sup>J. U. Trefny and B. Serin, *J. Low Temp. Phys.* 1, 231 (1969).
  - <sup>27</sup>H. Fenichel and B. Serin, *Phys. Rev.* 142, 490 (1966).
  - <sup>28</sup>N. A. Lurie, G. Shirane, and J. Skalyo, Jr., *Phys. Rev. B* 9, 2661 (1974).
  - <sup>29</sup>P. Korpium, W. Albrecht, T. Müller, and E. Lüscher, *Phys. Lett. A* 48, 253 (1974).
  - <sup>30</sup>J. A. Barker, R. O. Watts, J. K. Lee, T. P. Schafer, and Y. T. Lee, *J. Chem. Phys.* 61, 3081 (1974).
  - <sup>31</sup>J. A. Barker (private communication).
  - <sup>32</sup>R. K. Crawford, in *Rare Gas Solids*, edited by M. L. Klein and J. A. Venables (Academic, New York, 1975), Chap. 11.
  - <sup>33</sup>A. M. Tremblay and H. R. Glyde, *Phys. Rev. B* 11, 1728 (1975).
  - <sup>34</sup>K. F. Niebel and J. A. Venables, *Proc. R. Soc. Lond. A* 336, 365 (1974).
  - <sup>35</sup>M. B. Doran, *J. Phys. B* 7, 558 (1974).
  - <sup>36</sup>M. B. Doran and I. J. Zucker, *J. Phys. C* 4, 307 (1971).
  - <sup>37</sup>G. G. Chell and I. J. Zucker, *J. Phys. C* 2, 35 (1968).
  - <sup>38</sup>R. P. Feynman, N. Metropolis, and E. Teller, *Phys. Rev.* 75, 561 (1949).
  - <sup>39</sup>N. N. Kalitkin, *Sov. Phys. JETP* 11, 1106 (1960).
  - <sup>40</sup>E. E. Salpeter and H. S. Zapolsky, *Phys. Rev.* 158, 876 (1967).
  - <sup>41</sup>F. C. Auluck and Ashok Jain, *Phys. Rev. B* 1, 931 (1970).
  - <sup>42</sup>M. Ross and B. J. Alder, *J. Chem. Phys.* 47, 4129 (1967).
  - <sup>43</sup>J. L. Masse (private communication).
  - <sup>44</sup>D. J. Pastine and M. J. Carroll, Symposium on Acc. Charact. of High Pressure Environment, Natl. Bur. Stand., Gatherburg, Oct. 1968 (unpublished).
  - <sup>45</sup>D. L. Raimondi and G. G. Jura, *J. Phys. Chem. Solids* 28, 1419 (1967).